Volume 2, Chapter 15: Orbit Determination*

1. Introduction

An Earth satellite collecting GPS data with an onboard receiver can compute its state in a diversity of ways, the choice depending in part cm the type of orbit and mission requirements. Tracking and navigation requirements for a typical mission may include real time state knowledge and active control during launch and orbit insertion (Axelrad and Parkinson, 1989) and during rc-entry and landing; real time relative navigation between vehicles during rendezvous (Hesper et al., 1992; Axelrad and Kelley, 1986); autonomous stationkeeping and near real time orbit knowledge for operations and orbit maintenance (Chao et al., 1992); rapid post-maneuver orbit recovery (Lichten et al., 1993); and after-the-fact precise orbit determination for scientific analysis (Yunck et al., 1985; Schreiner et al., 1992). Orbit accuracy requirements can range from hundreds of meters or more for routine operations to a fcw centimeters to support precise ocean altimetry. Uniquely among existing tracking systems, GPS can meet the most stringent of these needs for the most dynamically unpredictable vehicles. An overview of GPS space applications is given in Munjal et al. (1992).

The GPS signal beamwidths extend roughly 3000 km beyond the earth's limb to enable an earth orbiter below that altitude to receive continuous three-dimensional coverage. Above 3000 km altitude, coverage begins to degrade. This chapter focuses on orbit estimation for satellites in low circular orbits, below a fcw thousand kilometers, with emphasis on the high accuracy that GPS so ably provides. Real time techniques fall under what wc shall call *direct* GPS orbit determination, in which only the GPS data collected by the orbiter are used in the solution. For precise after-the-fact solutions wc turn to a form of *differential GPS in* which data collected at multiple ground sites are combined with the user data to reduce the overall error. We also examine briefly the adaptation of GPS tracking techniques to satellites in highly elliptical and geosynchronous orbits.

The potential of GPS to provide accurate and autonomous satellite orbit de.termination was noted early in its development, for example, by Parkinson (1976). Early studies of direct GPS-based tracking include those by Farr (1979), who surveyed applications from near Earth to beyond geosynchronous altitudes; Van Leeuween et al. (1979), who examined GPS tracking of the Space Shuttle; Tapley (1980), who focused on autonomous near Earth navigation; Wooden and Teles (1980), who described NASA's first planned GPS orbital application to Landsat-4; Kurzhals and Fuchs (19'81), who compared the potential of GPS and NASA's Tracking and Data Relay Satellite System (TDRSS) for onboard navigation; Masson et al. (1 982), who discussed flight receiver requirements and expected onboard orbit accuracies from near Earth to geosynchronous altitude; and Jorgensen (1982), who addressed geosynchronous applications, The first reported results from direct GPS tracking were those of the Landsat-4 experiment (Heuberger and Church, 1983; f'ang and Seifert, 1985), which achieved approximately 20 m accuracy during the relatively brief periods of good GPS visibility at that time.

Among the first descriptions of precise orbit determination at the level of several decimeters or better by differential GPS techniques arc those by Ondrasik and Wu (1982), who proposed a sub-

* Thomas 1'. Yunck, Jet Propulsion Laboratory, California institute of Technology

decimeter carrier phase-based technique for the Topex (later Topex/Poseidon) ocean altimetry mission; Ananda and Chernick (1982), who examined differential tracking of a low altitude orbiter; Wu (1985), who proposed differential techniques for high altitude satellites; and Yunck et al. (1985), who surveyed a variety of differential GPS applications. Since then, several important refinements have been introduced which better exploit the unique signals anti the unprecedented observing strength GPS provides.

2. Principles of Orbit Determination

instantaneous point positioning with GPS pseudorange is about as accurate in low orbit as on the ground: typically 50-100 m for the SPS user (under nominal levels of selective availability) and 10-20 m for the PPS user. instantaneous velocity solutions derived from carrier phase rate may be accurate to 0.5 m/sec for the SPS user and better than 0.1 m/sec for the PPS user. While such solutions are adequate for many purposes, they have limitations. An instantaneous solution is impossible during data outages or periods of restricted visibility, for example, and its accuracy may be inadequate for orbit prediction or for some real time needs. Some scientific instruments require real time position knowledge of meters to tens of meters for accurate pointing, while after-the-fact requirements can be far more stringent. To reduce the instantaneous position and velocity error, the traditional tools of dynamic orbit estimation can be brought to bear.

a) Dynamic Orbit Determination

Classical dynamic orbit determination exploits orbital mechanics—the physics underlying orbital motion- and filtering theory to yield a well-cictcrmincci solution from generally sparse and noisy measurements. This approach has in fact been necessary with conventional tracking systems, which, unlike GPS, seldom if ever provide sufficient information at one time for a geometric solution, and can provide no measurements at all over much of the globe. (An exception is the usc of range and angle data from a single site to determine the instantaneous position of geostationary satellites, though the accuracy of that technique is far worse than with GPS.) An orbit model must therefore be introduced to supply the missing information. In dynamic orbit determination the orbit model is derived from models of the forces acting on the satellite and the laws of motion,

The process begins with a set of tracking measurements (range, Doppler, or angles, for example) along with mathematical models of the forces acting on the satellite anti of the satellite physical properties. The major forces include gravity, aerodynamic drag anti lift, solar radiation pressure, satellite thermal radiation, and active thrusting. Lesser contributions may come from leaks and outgassing, sunlight reflected from the earth, anti electromagnetic effects. The force and satellite models arc then used to compute a model of satellite acceleration over time, from which, by double integration, a nominal trajectory is formed, In principle, all that's then needed to produce the orbit solution is to determine the two vector constants of integration- –position and velocity at some time point- also known as the epoch state. That is done through an estimation procedure which finds the epoch state for which the resulting model trajectory best fits the tracking data, according to some opt imalit y criterion---usually minimizing the mean square fitting error. '1'0 improve the fit, one can simultaneously estimate various other model parameters, such as drag, solar radiation, or gravity model coefficients, or empirical parameters, such as nonspecific once- and twice-per-orbit accelerations. The resulting solution, however, is still a trajectory derived from force models, and

its accuracy depends on how faithfully those models, fixed or adjusted, describe the real forces acting on the satellite.

More formally, to construct a nominal or a priori satellite trajectory we begin with Newton's second law of motion

$$\mathbf{f} = m\,\mathbf{a} = m\,\ddot{\mathbf{r}} \tag{1}$$

or

$$\ddot{\mathbf{r}} = \frac{\mathbf{f}}{m} \tag{2}$$

where $\mathbf{r}$ is the satellite position vector. This fundamental equation of mechanics provides the dynamical constraint governing the orbit solution. The true accelerat ion rat any instant depends on the satellite position and velocity at that instant, and on many other parameters that characterize the forces at work. In the orbit solution, those parameters may take the form of spherical harmonic gravity coefficients, drag and lift coefficients, solar flux and reflectivity, a geomagnetic index, and so on. Let $(\mathbf{r}_o, \dot{\mathbf{r}}_o)$ be the true satellite epoch state to be estimated. We first select a nominal epoch state $(\mathbf{r}_{on}$, **roll),** perhaps from an instantaneous GPS state solution, and construct an acceleration model $\ddot{\mathbf{r}}_n(t)$ from the force and satellite models. The nominal trajectory m(t) is then generated by double integrat ion of the accelerat ion model,

$$m(t) = \int\int m(t) \quad dt \; -t \; \dot{\mathbf{r}}_{on} \; t + \mathbf{r}_{on} \tag{3}$$

The least squares solution procedure will then estimate corrections to the nominal epoch state (and, if dc.sired, to selected force model parameters) that bring the model trajectory into better agreement with the tracking data. If only the six-element epoch state and a few other parameters arc adjusted, as is commonly the case, then in principle only a relatively few measurements around the orbit arc needed to yield a well-dctcrmincd solution, and a sparse tracking network will suffice. This is the great power and appeal of dynamic orbit determination. Since the first days of space exploration this techn iquc has made practical the accurate tracking of Earth satellites and deep space probes.

Observe, however, that the resulting orbit solution depends intimately on the (possibly adjusted) acceleration model r,)(t). Where high accuracy orbits are required, high accuracy models must bc found. This can be enormously costly and may be a practical impossibility in the case of low altitude and maneuvering vehicles. In the mid-l 980s it was recognized that the continuous 3-D coverage provided by GPS offers an escape from this dynamical bind. Before describing the orbit estimation techniques, wc first review some principles of optima] estimation theory.

b) The Batch Least Squares Solution

A time-honored technique for estimating satellite orbits is the method of least squares, first employed by Gauss in 1795. Let $\mathbf{z}$ be a vector of tracking measurements $(z_1,\ldots,z_n)^T$ made over an interval of time, often called a tracking arc, The objective is to find the one trajectory among all possible trajectories satisfying the dynamical constraint (Eq. 2) which minimizes the mean square

difference between the actual observations z_i and theoretical observations $\tilde{z}_i$ derived from the solution trajectory. That is, we want to find the trajectory r(t) that minimizes the functional

$$J = \sum_{i=1}^{n} [z_i - \tilde{z}_i (\mathbf{r}(t))]^2 \tag{4}$$

As this is a nonlinear problem, we reformulate it as one of computing a linear correction to the nominal trajectory m(t) given by Eq. 3. First we compute theoretical observations $\tilde{z}_i$ from the nominal trajectory, then form the differences $\delta z_i = z_i - \tilde{z}_i$. These *prefit residuals* become the observations to be used in a linear adjustment of the nominal trajectory. (Strictly speaking, this is still not a linear problem; but if the nominal trajectory is sufficiently close to the true trajectory, it will be in the "linear regime," where a linear correction is adequate, if not perfect. If greater accuracy is needed, a linear correction to the new solution can be computed, and so on, until the solution converges.) The familiar linear equation can be written

$$\delta \mathbf{z} = A \mathbf{x} + \mathbf{n} \tag{5}$$

where **x** is the vector of parameters to be estimated, **n is** the vector of random measurement noise on the observations $\delta \mathbf{z}$, and A is a matrix of partial derivatives of the observations with respect to the elements of x. Here x includes at a minimum the adjustments to the six epoch state parameters, and may include adjustments to various dynamic and geometric model parameters as well. Equation 5 is called the regression equation and A is the matrix of regression coefficients.

A detailed discussion of the construction of A is beyond the scope of this chapter, but a simple overview is in order. An element a_{ij} of A is given by

$$a_{ij} = \frac{\partial z_i}{\partial x_j} \tag{6}$$

where, for simplicity, z_i now represents the differential element δz_i. This partial derivative relates an observation z_i at one time point to state parameter x_j at a possibly remote reference time. The A matrix thus contains the state transition information from the reference epoch to all times in the data arc and must therefore embody the dynamical constraint of Eq. 2. To compute the a_{ij} we first write

$$\frac{\partial z_i}{\partial x_j} = \frac{\partial z_i}{\partial \mathbf{x}_{ci}} \frac{\partial \mathbf{x}_{ci}}{\partial x_j} \tag{7}$$

where $\mathbf{x}_{ci}$ represents the satellite state at the time of observation z_i. This explicitly introduces the current state $\mathbf{x}_{ci}$ and its relation to both the current observation z_i and the epoch (and other) state variables x_j. The partial $\partial z_i / \partial \mathbf{x}_{ci}$ contains no dynamical information and can be computed directly. The partial $\partial \mathbf{x}_{ci} / \partial x_j$ relates the satellite state at the observation time to the epoch state and thus embodies the dynamical constraint. To determine that partial we differentiate the equation of motion (3) with respect to the epoch state parameters, producing a set of linear second order differential equations in $\partial \mathbf{x}_{ci} / \partial x_j$. These *variational equations* are then integrated numerically to obtain the partial derivative, and thus the final regression coefficients.

The well-known least squares solution corresponding to the regression equation **(5) is** given by

$$\hat{\mathbf{x}} = (A^T R_n^{-1} A)^{-1} A^T R_n^{-1} \mathbf{z} \tag{8}$$

Where

$$R_n = E[\, n\ \mathbf{n}^T] \tag{9}$$

is the covariance matrix associated with the measurement noise vector **n.** This is known as the batch least squares solution since it requires that all observations over a data arc be collected together and processed as a batch, In practice, when many parameters are estimated Eq. 8 will require large matrix inversions, which can give rise to serious numerical problems, Most orbit determination filters today therefore employ more stable techniques that we shall deal with shortly.

c) Kalman Filter Formulation

A spaceborne GPS applicat ion may require a cent inures real t i me st ate solution more accurate than point positioning can provide. Although filtering is needed to achieve this, a batch solution is generally inappropriate since it may require a long accumulation of measurements ant] a large amount of computation at once. In such cases a sequential estimator is called for, the most popular example of which is the Kalman filter.

A sequential filter continually updates the current state estimate with each new measurement. The computation needed for each update is small compared with that for a full batch solution (although for a properly formulated filter the computation required for many hours of updates is comparable to that for the same size batch solution); hence an onboard processor can maintain the solution in real time. It should be noted that the sequential current state estimate employs only data from the past up to the present, while a batch filter may estimate a state with data from both before and after an epoch. In non-real time uses the final sequential state estimate can be mapped to all times in the data arc, just as in a batch solution, to achieve an equivalent result.

The conventional Kalman filter is formulated in discrete time recursion relations. Suppose the filter has produced a state estimate $\hat{\mathbf{x}}_i$, at time t_i (using data up to and including time t_i), and that the estimated covariance matrix for $\hat{\mathbf{x}}_i$ is $\hat{P}_i$. The state solution $\hat{\mathbf{x}}_{i+1}$ at time t_{i+1} is derived in two steps: 1) the *time update*, in which a predicted or a priori solution $\tilde{\mathbf{x}}_{i+1}$ and covariance matrix $\tilde{P}_{i+1}$ arc generated from their values at time t_i, with no new data yet included, and 2) the *measurement update*, *in* which the new estimates $\hat{\mathbf{x}}_{i+1}$ and $\hat{P}_{i+1}$ are generated from the data at time t_{i+1}, as corrections to the predicted values.

The time update proceeds as follows:

$$\tilde{\mathbf{x}}_{i+1} = \Phi_i \hat{\mathbf{x}}_i \tag{10}$$

anti

$$\tilde{P}_{i+1} = \Phi_i \hat{P}_i \Phi_i^T \tag{11}$$

where Φ_i is the transition matrix, derived from the equation of motion, relating the state at t_i to the state at t_{i+1}. The measurement update is then

$$\hat{\mathbf{x}}_{i+1} = \tilde{\mathbf{x}}_{i+1} + G_{i+1} , (\mathbf{z}_{i+1} - A_{i+1} , \tilde{\mathbf{x}}_{i+1}) \tag{12}$$

and

$$\hat{P}_{i+1} = \tilde{P}_{i+1} - G_{i+1} A_{i+1} \tilde{P}_{i+1} \tag{13}$$

where $\mathbf{z}_i$ is the measurement vector at time t_i, A_i is the matrix of measurement partials with respect to $\mathbf{x}_i$, and G_i is the so-called Kalman gain, given by

$$G_i = \tilde{P}_i A_i^T (A_i \tilde{P}_i A_i^T + R_{ni})^{-1} \tag{14}$$

where R_{ni} is the error covariance of the measurement vector $\mathbf{z}_i$. (In some applications, for example where onboard computing may be limited, a subopt i mal *fixed gain* filter can be employed, in which G is predetermined.) Note from (14) that, like the batch formulation, the conventional current state Kalman filter formulation involves matrix inversion, which can lead to numerical instability. Various alternative approaches have been devised (e.g., Bierman, 1977 and Thornton, 1976) which employ *pseudoepoch state* factorized formulations. These avoid matrix inversion by factoring P into either upper triangular and diagonal matrices (U-D formulation) or its square-root matrices (square-root information filter or SRIF formulation). Factorized filters have been incorporated into several of NASA's high performance orbit determination systems. For more on these techniques see Lichten (1990) and the references therein.

Comparison of the batch and sequential formulations reveals that the latter is simply a recursive equivalent of the former. For a given data arc, the final sequential and batch solutions, when mapped to the same epoch with the final dynamical models, will be identical. As presented here, both arc dynamical formulations which depend fundamentally on physical force models to produce the solution trajectory. It is worthwhile at this point to examine the principal errors that arise in the dynamic state solutions.

d) Dynamic Orbit Error

For simplicity, let us consider only the PPS user and only position error. The typical accuracy of instantaneous point positioning with pseudorange is] 0-20 m, with the major errors resulting from GPS orbit and clock error, and pseudorange measurement error. Filtered solutions reduce these errors in three ways. First, random measurement error is smoothed against the dynamic model over the full fitting arc, with the resulting position error decreasing inversely as the square-root of time. Meter-level independent random errors can, after a few hours, be reduced to centimeters. At the same time, many systematic errors—GPS orbits and clocks, multipath—will be at least partly inconsistent with (orthogonal to) the user satellite dynamic models, and will be attenuated in the solution. (Errors that correlate strongly with orbital dynamics, such as once-per-orbit ionospheric effects, may remain at full force.) Finally, dynamic information is introduced which supplements (and may dominate.) the geometric information in the point position solution. Dynamic orbit accuracies of a few meters might therefore be achieved. A number of groups now distribute GPS

orbit and clock solutions that are accurate to better than 1 m. When those rather than broadcast data arc used, the filtered user state error can fall below 1 m.

This error reduction does not come for free: As the dynamic filter smooths measurement error, it introduces dynamic mode] error. Since force models arc imperfect, the integrated model trajectory will be imperfect as well. Force model adjustments made as part of the solution may offer little improvement. And since the dynamic solution yields a trajectory derived from the final force models, residual errors in those models become errors in the solution trajectory. Gravity and drag model errors are often dominant, and both increase rapidly as the satellite altitude is reduced. Thus accurate dynamic orbit determination becomes problematical at low altitudes. To take some examples, the motion of Lageos, a dense, inert sphere at about 6000 km altitude, can be modeled to within a few centimeters over periods of weeks; the motion of Topcx/Poseidon, a much larger vehicle at 1336 km, to about 10 cm over 10 days; the motion of SEASAT, at 800 km, to one or two mete.rs over one day; and the motion of the Shuttle, at 300-400 km, to no better than tens of meters over an orbit. At low altitudes, therefore, dynamic filtering may offer little. or no advantage over simple point positioning,

Dynamic model errors often reveal themselves as signatures in the post-fit residuals; that is, they create systematic discrepancies between the actual measurements, which reflect the true trajectory, and theoretical measurements derived from the solution trajectory. We can imagine an extreme case in which a force varies randomly from one time step to the next and is therefore inherently unpredictable, but can be observed in the residuals. At some level, a number of forces (e.g., drag, gravity anomalies) can appear to behave that way. What is needed, then, is a means of exploiting information in the residuals to correct the orbit solution. The Kalman filter provides such a means in the form of process noise modeling.

e) Kalman Filter with Process Noise

Augmenting a Kalman filter with a process noise model is a way of telling the filter that the information in Φ and A describing the behavior of the state is incomplete---that there is a component of that behavior for which the filter has no model, which it cannot predict, but which it may be able to observe in the data. This unknown behavior is modeled in the filter as a stochastic process (though in reality it maybe deterministic). The filter then tries to detect that behavior in the measurements and track it at each time step.

in the context of orbit determination this means that at each time step, in addition to applying the standard dynamic updates, the filter will examine the discrepancy between the dynamic state estimate and the apparent state as indicated by the measurements. From that discrepancy it will estimate. a local correction to the dynamic model, valid oniy over the update interval (t_{i-1}, t_i). When added to the dynamic model, that correction will reduce the disagreement between the observations and the solution trajectory at time t_i. As it proceeds through the data, the. filter will generate a sequence of local force model corrections, one at each update, time, bringing the solution trajectory into better agreement with the observations. That may be good or bad, depending on the quality of the observations and the accuracy of the models. We will therefore want to take care to hinder the local corrections from chasing after bad measurements.

The process noise model can take many forms, and various constraints may be applied to limit the freedom of each new correction to depart from the dynamic model or from the previous correction. in practice, the stochastic correction is often introduced by augmenting the state vector $\mathbf{x}_i$ with a parameter vector pi representing the local force model adjustment to be estimated at time t_i. For this discussion we will let $\mathbf{p}_i=(p_{i1}, p_{i2}, p_{i3})^T$ denote a 3-D force which is constant over the interval (t_{i-1}, t_i) and zero elsewhere. This force will be estimated to account for any discrepancy between the dynamic solution update and the observations at time t_i, and this will be repeated at all time steps. The augmented state vector $\mathbf{X}$ thus has three additional elements

$$\mathbf{X} = \begin{bmatrix} \mathbf{x} \\ \mathbf{p} \end{bmatrix} \tag{15}$$

An effective realization of the process noise sequential filter used extensively by NASA in orbit estimation is given below (Bierman, 1977; Wu et al., 1986),

Time Update:

$$\tilde{\mathbf{X}}_{i+1} = \Phi_i \hat{\mathbf{X}}_i \tag{16}$$

and

$$\tilde{P}_{i+1} = \Phi_i \hat{P}_i \Phi_i^T + B Q_i B^T \tag{17}$$

where now wc have

$$\Phi_i = \begin{bmatrix} \Phi_x(i+1,i) & \Phi_{xp}(i+1,i) \\ 0 & M_i \end{bmatrix} \tag{18}$$

$$\mathbf{B} = \begin{bmatrix} \mathbf{0} \\ \mathbf{I}_p \end{bmatrix} \tag{19}$$

Φ_x is the dynamic transition matrix of Eq. 10; $\Phi_{xp}(i+1,i)$ is the transition matrix relating $\hat{\mathbf{x}}_{i+1}$ to the process noise parameters $\mathbf{p}_i$; M_i is a 3x3 diagonal matrix with the jth element

$$m_j = \exp\ [-(t_{i+1} - t_i) / \tau_j] \tag{20}$$

Q_i is a diagonal covariance matrix associated with a white noise process, with the jth element

$$q_j = (1 - m_j^2)\, \sigma_j^2 \tag{21}$$

and $\mathbf{I}_p$ is a 3x3 identity matrix. The measurement update equations arc identical to (12)-(14), except that now wc use the augmented state vector' X and its associated covariance matrix P.

This is a first-order Gauss-Markov process noise model. Note that M_i is the transition matrix for the process noise parameters, and that the transition is in the form of a decaying exponential correlation. 'l'he time constant τ_i in (20) can be chosen to reflect the correlation in the dynamic modeling error (and thus in the desired correction) over one update interval. If τ_i is much smaller than the update interval, then m_i is small; the model error is therefore regarded as uncorrelated from batch to batch, and this becomes a white noise error model. ~'here is one other selectable parameter, the steady state variance σ_i^2. Through Eq. 21, σ_i^2 scales the batch-to-batch variance q_i, which further constrains the correction. In the case of a white noise model, this constrains each independent correction with respect to the dynamic model, with no dependence on the previous correction, If σ_i=0, the local force correction is constrained to zero and the conventional dynamic solution is obtained. in summary, the real constraint is determined by τ_i (through m_i) and σ_i^2 as they combine through (21) to form the weighting matrix elements q_i.

Stochastic force models introduce an additional complication for non-real time applications in which an optimal solution over an entire data arc is desired. It is no longer sufficient simply to map the final state solution to other times by means of the final dynamical models. The local force corrections have been determined with data only up to the times they occur, and thus have not benefitted from later measurements. To complete the estimates of the local forces it is necessary to filter the data in the reverse direction as well, a process called smoothing, before mapping to all time points. The combined estimator is known as a filter/sn~oothcr.

With conventional (sparse) tracking data one must be careful when employing process noise mode] corrections. The data acquired at any one time are often weak (or nonexistent), and insufficient by themselves to determine position. A relaxed constraint on the process noise estimate may result in a large and erroneous adjustment to the state, or may cause the solution to fail. Care must be taken to constrain the corrections within the observability limits of the data. This has traditionally meant relatively long correlation times and tight batch-to-batch sigmas.

3. Orbit Estimation with GPS

We arc now in a position to examine the powerful advantages GPS brings to estimating satellite orbits. First we'll look at a purely geometric technique that can improve dramatically upon point positioning accuracy, without any dynamic filtering, by combining the continuous carrier phase and pseudorange observable.

a) Carrier-Pseudorange Precise Posit ioning

When pseudorange and continuous carrier phase arc brought together, the basic method of geometric point positioning can be refined to track the position of an arbitrarily moving vehicle with high accuracy. The technique is analogous to estimating a carrier phase bias by averaging the difference between continuous phase and pseudorange. This converts biased phase to a precise pseudorange with a small residual bias, preserving the detailed information on range change in carrier phase. More generally, we can construct a biased record of 3-D position change from nlLllti-satellite carrier phase, then estimate the 3-D position bias by averaging the point-by-point vector difference between that record and corresponding point position solutions.

The concept is illustrated in Figs.1 a-c. A sequence of N independent point position solutions $\hat{\mathbf{x}}_k$ is shown in Fig 1a. The true receiver motion is represented by the dashed line. If $\mathbf{x}_k$ is the true position at time t_k, wc can write

$$\hat{\mathbf{x}}_k = \mathbf{x}_k + \mathbf{n}_k \tag{22}$$

where, for simplicity, wc assume $\mathbf{n}_k$ is a white noise process with diagonal covariance elements σ_{nj}^2, j= 1,2,3. Figure lb shows the record of position change obtained by tracking carrier phase over the same arc. This is a precise representation of the true path, but with an arbitrary offset in position. It can be regarded as a series of position estimates, $\bar{\mathbf{x}}_k$, having a small random error and an arbitrary common bias:

$$\bar{\mathbf{x}}_k = \mathbf{x}_k + \mathbf{b} + \mathbf{e}_k \tag{23}$$

where $\mathbf{b}$ is the bias vector and $\mathbf{e}_k$ is a white noise vector having diagonal covariance elements σ_{ej}^2. We estimate the bias $\mathbf{b}$ by averaging the difference between the $\bar{\mathbf{x}}_k$ and $\hat{\mathbf{x}}_k$:

$$\hat{\mathbf{b}} = \frac{1}{N}\sum_{k=1}^{N} \bar{\mathbf{x}}_k - \hat{\mathbf{x}}_k \tag{24}$$

01
$$\hat{\mathbf{b}} = \mathbf{b} + \frac{1}{N}\sum_{k=1}^{N} \mathbf{e}_k - \mathbf{n}_k \tag{25}$$

Since σ_{ej} is typically 100 times smaller than σ_{nj}, the approximate component error on the bias estimate is

$$\sigma_{\hat{b}j} \cong \frac{\sigma_{nj}}{\sqrt{N}} \tag{26}$$

Thus meter-]cvc] random noise on 1-scc pseudorange data can give a decimeter-level bias estimate within 2 rein, and a centimeter-level estimate within a few hours. (We ignore GPS ephemeris and clock error, which are treated in later sections.) Subtracting Eq. 25 from Eq. 23 eliminates the position bias in the phase solution to give a precise record of absolute position. As shown in Fig. 1 c, the final path solution sits close to, and has nearly the exact shape of, the true path. The final positions will have an approximate component error

$$\sigma_x = (\sigma_{\hat{b}}^2 + \sigma_e^2)^{1/2} \tag{27}$$

where $\sigma_{\hat{b}}$ represents the residual bias common to all points and σ_e is the point-to-point random error. The solution path therefore has the precision and time resolution of a pure carrier solution, with an absolute bias that is a fraction of the point position error.

This technique is well suited to real time recursive execution. Consider a receiver that produces an instantaneous point position $\hat{\mathbf{x}}_k$ at time t_k, and position change $\Delta\hat{\mathbf{x}}_k$ obtained from carrier phase tracked from t_{k-1} to t_k. An unbiased estimate $\hat{\mathbf{X}}_{n+1}$ of the position at time t_{n+1} is given by:

$$\hat{\mathbf{X}}_{n+1} = \frac{n}{n+1}(\hat{\mathbf{X}}_n + \Delta\hat{\mathbf{x}}_{n+1}) + \frac{1}{n+1}\hat{\mathbf{x}}_{n+1} \quad \textbf{(28)}$$

This is a variation on the recursive formula for a simple average:

$$\bar{P}_{n+1} = \frac{n}{n+1}\bar{P}_n + \frac{1}{n+1}P_{n+1} \quad (29)$$

The position change information, $\Delta\hat{\mathbf{x}}_{n+1}$, maps the current position estimate $\hat{\mathbf{X}}_n$ forward to the next time point for averaging with the point position $\hat{\mathbf{x}}_{n+1}$ computed at that time, Carrier phase, in effect, inertially aids the sequential averaging of point position solutions to refine the phase bias estimate. The procedure can be tuned by weighting each $\hat{\mathbf{x}}_k$ by its inverse covariance.

A principal virtue of this technique is its extreme simplicity. A filter to precisely track unpredictable motion (or the relative positions of multiple vehicles) can be realized in a few lines of code. One drawback is its exclusion of external information about platform dynamics, making the solution vulnerable to outages which might easily be bridged with dynamic models. This is remedied in a more robust technique that employs the Kalman filter formalism.

b) Kinematic Orbit Determination

When a Kalman filter is applied to GPS data from a low orbiter, the full advantage of continuous 3-D coverage may not be realized without an aggressive use of process noise corrections. If we assume a full GPS constellation, a flight receiver having six or eight parallel channels, and a relatively wide field of view, strong instantaneous observing geometry is assured. Inclusion of continuous carrier phase data vastly increases the potential precision of the estimates. It then becomes possible to relax or eliminate constraints on the process noise force corrections and track the true motion of the vehicle with great precision.

The concept is illustrated in Fig. 2. The dashed curve represents the irregular path of a low orbiter subject to varying forces. With GPS data collected by the orbiter, we can execute a traditional dynamic orbit solution to produce the smooth orbit estimate shown by the solid line. This leaves a set of (possibly large) post-fit residuals. Because GPS provides continuous 3-D coverage, the post-fit residuals at each time point suffice to reconstruct the observed satellite position (its departure from the dynamic solution) by purely geometric means. The observed trajectory can then be constructed by adding the geometrically determined correction to the dynamic solution at each time point, Force model error, reflected in the initial post-fit residuals, is thereby eliminated.

This can be thought of as two distinct steps: First, a conventional dynamic solution produces a reference trajectory and post-fit residuals; the residual path is then constructed geometrically, point by point, and added to the dynamic solution, in practice this can be done in one estimation step in a Kalman filter with process noise. The estimated process noise parameters p in Eq. 15 can provide the geometric corrections to the dynamic solution. In ordinary tracking applications those parameters would be tightly constrained and geometric information only weakly expressed. But

the full observability offered by GPS allows all constraint to be removed. The correlation time τ_i can be set to zero (white noise model) and the steady state variance σ_i^2 to a large value. The filter will then estimate a 3-D force correction for each interval (and a corresponding change in the current state) to exactly account for the geometric discrepancy between the measurements and the dynamic solution. 'I'his is called non-dynamic or *kinematic* orbit determination, though both terms arc somewhat misleading since the technique builds on an underlying dynamic formulation.

As wc shall see in more detail later, the kinematic solution can be carried out with pseudorange data alone, with carrier phase data alone, or with the two in combination, Observe, however, that as the dynamic constraint is relaxed to allow the geometric correction, the effect of measurement error increases. Instead of being smoothed against the dynamic model, single-point measurement error is fully expressed in the geometric correction. Thus when pseudorange alone is used, the solution becomes a series of point positions with full pseudorange noise. For precise applications continuous carrier phase is therefore essential. Although this resembles the purely geometric technique of carrier-pseL)ctorangc positioning, the Kalman filter formulation, with its dynamic core, is inherently stronger and permits a highly accurate kinematic solution with carrier data alone.

c) Reduced Dynamic Orbit Determination

Because the kinematic correction is geometric, it is vulnerable to weak geometry. Momentary data outages or large PDOPs will cause the error to grow or the solution to fail. It may be noted, moreover, that the kinematic so] ution makes little use of dynamic information--it is an empirics] result constructed from the measurements. Often, however, useful dynamic information is at hand which, properly combined with geometric information, can improve the result. When geometry weakens or fails, dynamic information can then carry the solution with high accuracy.

We can achieve a balance of dynamic and geometric information in the orbit solution by imposing a judicious constraint on the process noise parameters. In an optimal solution (under the assumption of a Gauss-Markov process noise model) the time constant τ_i will reflect the actual correlation time of dynamic model errors, and the steady state variance σ_i^2 the actual error in the dynamic model. The geometric corrections will not be free to follow the measurements wherever they lead, but will be bound by the constraint to the dynamic model. Relative weight will in fact shift back and forth between dynamic and geometric information as observing strength varies. When geometry is weak, the process noise constraint will hold the correction close to the dynamic solution; if there arc no observations at all, no correction can be computed and the dynamic solution is produced. This opt i mized technique is known as *reduced dynamic* orbit determinat ion.

Another interpretation is given in Fig. 3, which illustrates the relative significance of random and systematic error in the solution trajectory. In the dynamic solution, random error is minimized (since the fewest parameters arc adjusted) while dynamic error is fully expressed. This is reversed in the kinematic solution as many parameters are adjusted, amplifying the effect of data noise while absorbing dynamic error. The reduced dynamic solution seeks the optimal balance to minimize overall error. We note, however, that minimum error is not always the first objective. For some science applications it may be desirable to convert systematic error to random error (kinematic solution) or vice versa (dynamic solution), even if the total error is not minimized.

This raises **the** question of how one chooses the process noise weighting. Often there is some prior knowledge of the quality of the force models in use and the consequent position error expected. Computer simulations or covariance analysis can then suggest a reasonable a priori weighting. When real data become available, a variety of strategies for tuning the reduced dynamic constraints become possible. One approach is simply to observe the magnitude of the process noise corrections. If they are near or exceed the constraints, the constraints should be relaxed; if they fall well short, the constraints can be tightened. Another technique is to compare contiguous orbit solutions at common end points (or on short overlapping segments) and then tune the constrains to maximize the agreement.

The reduced dynamic technique is one realization of the concept depicted in Fig. 2; many others are possible, For example, we might directly compute position rather than force corrections. An approach along those lines proposed by Wu (1992) has certain advantages (and is currently being exploited) for gravity recovery. Force corrections, however, directly augment the dynamic model and have the virtue that, although discontinuous (piecewise constant) themselves, they yield a continuous trajectory when integrated.

d) Orbit Improvement by Physical Model Adjustment

The reduced dynamic solution introduces local force model corrections to reduce the effects of dynamic model error. often it is more efficient to reduce that error by adjusting physical model parameters; fewer adjustments may be needed and data strength preserved. Adjustment of drag coefficients and radiation pressure terms (for both received solar radiation and emitted thermal radiation), for example, is common. Particularly attractive with GPS tracking data is *gravity fining*, or adjustment of gravity field coefficients. The geopotential is commonly represented as a spherical harmonic expansion containing anywhere from a few terms to a few thousand terms, depending on the fidelity required, In contrast to process noise parameters, which are local, each gravity harmonic is a global function representing a permanent component of the geopotential.

Many global gravity models have been derived from historical satellite tracking data, which is often sparse in some regions. GPS, however, leaves no coverage gaps. Since a polar orbiter overflies the entire globe, GPS tracking of such a satellite can enable permanent improvement of the global gravity model. That improvement will in turn reduce the dynamic error and permit tighter constraints on the process noise models in subsequent orbit solutions. Gravity tuning has elements in common with reduced dynamic orbit estimation: Both techniques adjust a large number of force parameters to bring the solution trajectory into closer agreement with the data, Where gravity is the dominant model error, gravity tuning is a desirable first step, since it yields a permanent model improvement.

4. Direct Orbit Determination with GPS

Sophisticated estimation strategies may be of little value in direct GPS-based orbit determination, where only the onboard GPS observables and broadcast data are used in the orbit solution. Although measurement noise can be reduced to centimeters by filtering, final user orbit error will be dominated by GPS ephemeris and clock error (with possibly large contributions from the ionosphere and selective availability for the SPS user) at a level of meters to tens of meters. While

dynamic filtering can mitigate those errors, evaluating the expected accuracy of the resulting solution is not straightforward.

Consider the batch least squares dynamic solution of Eqs. 8-9. It is easily shown that the error covariance P_x on the estimate $\hat{\mathbf{x}}$ is given by

$$P_x = -(A^T R_n^{-1} A)^{-1} \tag{30}$$

This is the formal error due to the random measurement noise vector **n** (Eq. **5), sometimes** called the commission error, It does not take into account other errors present in the solution, such as those due to GPS orbit and clock errors, sometimes called *omission* errors. To examine the effect of such errors we can include the relevant parameters and their relation to the observations explicitly in the regression equation (5) by writing

$$\delta \mathbf{z} = A\mathbf{x} + B\mathbf{y} + \mathbf{n} \tag{31}$$

where y is the vector of omission error parameters and B is a matrix of partial derivatives of the observations $\delta \mathbf{z}$ with respect to y. When the solution given by (8) is applied to (31) we have

$$\hat{\mathbf{x}} = \mathbf{x} + (A^T R_n^{-1} A)^{-1} A^T R_n^{-1} B\,\mathbf{y} + \tilde{\mathbf{n}} \tag{32}$$

where $\tilde{\mathbf{n}}$ is the transformed random measurement noise. "l'he long coefficient in front of y in (32) describes the response of the estimate $\hat{\mathbf{x}}$ to the error parameters y, and is called the sensitivity matrix, S, where

$$S = (A^T R_n^{-1} A)^{-1} A^T R_n^{-1} B \tag{33}$$

The total error covariance, $\mathbf{P}_{tot}$, of the estimated vector $\hat{\mathbf{x}}$ is given by

$$P_{tot} = P_x + S\ P_{om}\ S^T \tag{34}$$

where P_{om}, the a priori covariancc matrix for the omission errors, must be derived through careful analysis of those errors,

Since many omission errors arc physically unrelated and can be regarded as uncorrelated, P_{om} can often bc (and almost invariably is) set up as a diagonal matrix. The errors on the elements of a dynamic satellite state solution, however, are strongly correlated, (Note, for example, that there is a direct relationship between satellite altitude and in-track velocity; in a dynamic solution, an error in one will appear as a compensating error in the other.) **A** diagonal covariance matrix is therefore inadequate to assess the effect of GPS ephemeris error on a dynamic user orbit solution, and in fact can be shown to give a highly pessimistic estimate of the error that actually arises. To evaluate the effect of GPS orbit error on a dynamic user solution, a full covariance matrix is needed for the GPS state parameters. One way to obtain such a matrix is to simulate the GPS orbit determination process as it is carried out with ground data to produce the GPS orbits available to the user.

Such a study was done by Bertiger and Yunck (1990), The results showed that errors in the GPS orbits were attenuated by roughly a factor of two in the dynamic solution for a low orbiter at 1300 km altitude. That is, GPS orbit errors of 1 m resulted in errors of about 0.5 m in the user orbit. (When a diagonal GPS covariance matrix was used, this error was overestimated by a factor of about twenty.) Because the satellite under study was at the relatively high altitude of 1300 km, model error was at the decimeter level and the full benefit of dynamic smoothing could be gained. With a typical GPS broadcast ephemeris error of 5 m, wc could expect to achieve a dynamic real time solution for such a satellite accurate to 2-3 m, limited by the GPS orbit error.

At lower altitudes, dynamic modeling error grows. At 500 or 600 km dynamic error may roughly equal GPS ephemeris error. Below 500 km, user dynamic error may dominate, and the optimal filter will therefore deweight dynamics. For the Space Shuttle at 300 km, the optimal weighting will be almost purely kinematic; the Shuttle position error will therefore be essentially the range error (dominated by GPS orbit error) times the PDOP. Because GPS orbit errors change slowly, the direct kinematic error will be highly correlated from one second to the next.

The most accurate direct orbit solutions are therefore obtained by dynamic filtering for satellites above about 800 km (and below 3000 km), with the accuracy limited by GPS orbit error. The best GPS orbits produced today (available typically several days after the fact) are accurate to better than 1 m. in principle, such accuracies can be achieved nearly in real time. Moreover, accuracies of 1-2 m can be reached for GPS orbits and clocks predicted several hours into the future (Lichten and Bertiger, 1989), and thus available for true real time use. If dynamic filtering reduces the resulting user error by a factor of two above 800 km, real time dynamic tracking could be made accurate to about 1 m. At the lowest altitudes, where the kinematic solution is optimum, accuracy under these conditions would reach a few meters. For further improvement at all altitudes we must introduce a means of reducing GPS orbit error.

5. **Precise Orbit Determination with GPS**

A few classes of mission require orbit accuracies ranging from 1 m (land altimetry, precise imaging) down to a few centimeters (ocean altimetry, gravity field modeling). For that level of performance we turn to the techniques of differential GPS. As it has been developed for scientific precise orbit determination, differential GPS is intended for non-real time applications and differs considerably from the real time differential techniques used for regional navigation.

a) Global Differential Tracking

The fundamental concept is illustrated in Fig. 4. In addition to the flight receiver, a network of reference receivers around the world continuously tracks all GPS satellites in view. It is essential that the flight receiver and at least one ground receiver share common visibility of several GPS satellites at all times. If they are well distributed, only about six ground sites are needed to ensure this, though in recent experiments with Topex/Poseidon a dozen or more have been used. Several ground receivers maybe at *fiducial* sites—sites with accurately known absolute positions that will be held fixed during the solution. The best current ground site positions (for example, those of the

International Terrestrial Reference Frame maintained by the International Earth Rotation Service in Paris) are known relatively to 1-2 cm, and absolutely (with respect to the geocenter) to about 3 cm.

Pseudorange and carrier phase data from the flight and ground receivers are processed together to produce a single grand solution. The solution strategy can vary greatly in detail, but typically includes estimation of all GPS satellite orbits; the user orbit; transmitter and receiver clock offsets; all carrier phase biases; non-fiducial ground site positions; atmospheric delays at ground sites; and atmospheric drag, solar radiation pressure, and other satellite force parameters. Data arc lengths may range from a few hours to many days. Because only the fiducial sites are held fixed in the solution, they establish the reference frame in which all other positions are determined.

One variation permits *all* ground sites to be adjusted within a moderate constraint, typically 10-1000 m on each site. This severs the tic to a predetermined reference frame and allows the entire solution to rotate within the limits of the overall constraint. The solution is then mapped into a chosen reference frame (such as ITRF) through a seven-parameter transformation (translation, rotation, and scale) which minimizes the 3-D RMS difference between all ground site solutions and their values in the chosen frame. This removes dependence on a particular subset of sites to define the reference frame and reduces reference station error in the total error budget. A less powerful variation processes the ground and user data separately. The ground data first determine accurate GPS orbits and clock offsets, which are then applied in a direct user solution. This dots not exploit the parameter correlations that arise in the true simultaneous solution, and hence dots not achieve the same degree of error reduction, but may offer greater flexibility and convenience.

While global differential tracking constitutes a major logistical departure from direct tracking, the basic filter equations needed to carry it out (Eqs. 16-21) remain unchanged. What changes is the definition of the estimated state vector X. To the user state and other adjusted parameters we now append state elements for all GPS satellites, clock offsets for all transmitters and receivers, ground site positions, atmospheric delays, and so on. The matrices of measurement partials and a priori covariance are correspondingly augmented, and the solution becomes more computationally demanding. It is worth examining in more detail how some of the key parameters are treated.

b) Fine Points of the Global Solution

When carrier phase data are used in a grand solution, either alone or together with pseudorange, the effective data noise (random measurement error) is typically below 1 cm. This can be seen in the post-fit residuals of global geodetic solutions, which for the combined dual frequency phase observable arc typically 3-6 mm. As revealed in numerous covariance studies (Eq. 24), random measurement error will contribute on the order of 2-3 cm (o the user position error-- somewhat higher for purely kinematic solutions and lower for purely dynamic solutions. In the grand solution, the major systematic mode] errors that plague the direct solution (GPS orbits and clocks) arc reduced, Note, however, that if GPS satellite dynamics and clocks are poorly modeled, the G1'S orbit and clock estimates will degrade and systematic errors will still arise in the user state solution. Fortunately, the high-altitude GPS satellite dynamics can be well modeled over 24 hrs, and standard dynamic GPS solutions generally suffice. For longer arcs, a weak stochastic adjustment of the GPS solar pressure parameter may be required.

For clock solutions we have several options. If high quality atomic clocks are used in all receivers and transmitters, simple quadratic models might suffice over many hours. Because, real clock behavior can be unpredictable, common practice is to allow for the worst by solving for all clock offsets independently at each time step under a loose constraint. 'l'his is equivalent to modeling clock behavior as a white noise process with large variance, in analogy with our treatment of the process noise state parameters in the kinematic orbit solution, It is also similar to the popular practice of double differencing to eliminate clock parameters; however, when global data sets are used, as they must bc for precise orbit determination, the white noise clock model is more powerful, as it retains more data (Wu, 1984). Just as purely kinematic orbit determination fails to exploit known dynamics of the satellite, white noise clock models fail to exploit known (and perhaps very smooth) clock behavior, and thus must be regarded as a conservative strategy.

Computer simulations, covariance studies, and results with Topcx/Poseidon have shown that the grand solution strategy can reduce user satellite position errors due to GPS orbit and clock errors to a fcw centimeters. What then becomes the dominant error in the user solution? one candidate is the error in modeling atmospheric propagation delay at the ground sites---or, rather, the variable, wet component of that delay. When standard seasonal models (supported by surface weather data) arc used to calibrate the atmospheric delay, the error is typically 3-5 cm at zenith, which may translate into 2-10 cm of user state error, depending on the solution technique. This can be reduced by periodically solving for a zenith delay at each site. The most powerful strategy yet developed is to model the zenith delay as a stochastic process (a random walk, for example) and adjust it at each time step under a constraint derived from the observed power spectrum of atmospheric delay variation, Typical zenith delay acc uracies with this technique are about 1cm.

Finally, wc note that each carrier phase observable contains an arbitrary bias corresponding to integer cycle ambiguities at each frequency. Those biases must bc estimated (or eliminated by time differencing) whenever the phase observable is used, In precise ground-based geodesy, an effort is often made to determine the exact integer cycle ambiguities in the differential observables and then fix the biases at those values. Resolving ambiguities between an orbiter and ground sites is demanding and, when many hours of data are used, can be shown to contribute little to solution strength, since at that point data noise is not a dominant error. The differential strategies described here attempt no cycle ambiguity resolution, and instead treat each bias as a continuous variable in the grand solution.

c) Precise Orbit Determination Performance Analysis

It should now be evident that the general strategy for achieving high accuracy with GPS is to exploit the great strength of GPS data to observe and correct any systematic errors that threaten to dominate. Just how the data will stand up to this demand depends on many details of system configuration and solution strategy. To illustrate those dependencies, wc present the results of computer covariance studies for severs] real or proposed missions. All studies include both commission and omission errors in an attempt to arrive at realistic final error estimates.

The first example is taken from error studies conducted for Topex/Poseidon years in advance of its launch in August of 1992. Topex/Poseidon is a U.S.-French ocean altimetry mission flying at an altit ude of 1336 km, where dynamic model errors are now well below 10 cm. The GPS

configuration for "1'opcx/Poseidon includes a six-channel (dual frequency) flight receiver with a hemispherical field of view, and a six-site ground network. The assumptions, error model, and estimation strategy arc summarized in Table 1. Note that a reference frame error of 5 cm per component for each of three fiducial sites was assumed, far greater than that error today.

Figure **5 shows** the predicted RMS altitude error for three solution strategies— dynamic, kinematic, and optimized reduced dynamic-as a function of the gravity model error, Because the kinematic solution eliminates dynamic error, it is independent of the gravity model. Its total error is divided almost equally between data noise and reference site error (which will virtually disappear with the free network strategy). The dynamic solution error depends strongly on gravity error and becomes limited by data noise and reference frame errors only when gravity and other dynamic model errors approach zero. 'l'he optimized reduced dynamic strategy surpasses both kinematic and dynamic— the latter even when the gravity error is zero, since other dynamic errors will still be reduced.

Also shown in Fig. 5 are three dots representing actual results from Topex/Poseidon obtained during the first year of the mission. The dots give the RMS altitude agreement between purely dynamic solutions made with ground based laser ranging and Doppler data, and the GPS reduced dynamic solutions. An RMS agreement of about 6 cm was obtained with the final prelaunch gravity model, known as JGM-1, which has a quality roughly in the center of the range shown. This agreement improved to about 3.5 cm when the JGM-2 model, which had been tuned with laser and Doppler tracking data, was produced by the Goddard Space Flight Center several months after launch (Yunck et al, 1993). 'l'he agreement improved further, to about 2.5 cm, when the JGM-2 model was tuned with the more comprehensive GPS data by investigators at the University of Texas (Schutz et al, 1993). At this point the RMS altitude error resulting from gravity mismodeling is believed to be no more than 2 cm.

Past ocean altimetry missions have been plagued by what arc known as geographically correlated orbit errors---that is, orbit solutions that arc consistently biased in different geographic regions, Such errors can confound the construction of global circulation models from the altimetry data. Geographically correlated orbit errors are often a consequence of geographic biases in the gravity model, although other factors may also play a role. Studies by Rosborough and Mitchell (1990) showed that kinematic and reduced dynamic orbits, by reducing dependence on force models in general, can virtually eliminate any geographic correlation in orbit errors resulting from the gravity model. That result was dramatically confirmed with l'opcx/Poseidon, 1,aser/Doppler dynamic orbit solutions with JGM-1 showed consistent and pronounced geographic discrepancies from the GPS reduced dynamic solutions. In later dynamic solutions employing the GPS-tuned gravity model, geographic discrepancies had all but vanished.

A second example is taken from the Earth Observing System, a suite of scientific Earth probes planned to fly at about 700 km, beginning in the late 1990's. Because dynamic errors may grow large at that altitude, a purely kinematic analysis is presented, This time the reference site error is reduced (o 3 cm per component. Other assumptions that differ from the Topex/Poseidon analysis arc shown in Table 2. Figure 6 shows the resulting predicted altitude error as a function of data arc length for several different GPS data combinations. The data type called "carrier-quality range" is a fictitious pseudorange measurement having the precision of carrier phase, and serves to establish a performance bound.

Figure 6 indicates that few-centimeter accuracy is possible for dynamically complex platforms, and that even the biased carrier phase observable used by itself can approach the performance of the strongest possible data type, It may seem surprising (hat the kinematic solution can succeed with carrier phase alone, since lhc grand solution must estimate phase and clock biases, and those biases are nicely constrained by pseudorange data. But the dynamic core of the kinematic sol ution allows the biases to be reliably estimated, just as they are in any integrated Doppler dynamic solution. This illustrates a fundamental difference between the process noise Kalman filter formulation and the simple carrier-pseudorange bias estimation of Sect. 3-a. The latter depends entirely on pseudorange to provide an absolute phase bias estimate, while the former can recover the bias dynamical] y (while correcting the model kinematical y) when range information is absent,

A third study explores the limits of kinematic performance with a stringent tracking challenge: the Space Shuttle at 300 km. For a given phase noise, kinematic tracking accuracy is limited largely by observing geometry, which wc strengthen by assuming a full sky field of view (each Shuttle is equipped with GPS antennas top and bottom to permit this), a flight receiver able to track all satellites in view (typically 13-15), and eleven ground sites, with reference site error of 1.5 cm pcr component (about what it is believed to bc in 1994). Other assumptions are given in "l'able 3. As shown in Fig. 7, the limiting error in a]] components now approaches 1 cm, though in reality dynamic errors in the GPS satellite orbit sol utions may degrade this somewhat. This opens up new possibilities for near-earth ocean altimetry and other precise Earth observations on platforms of opportunity, and for short-duration testing of precise instruments on the Space Shuttle.

d) Single-Frequency Precise Orbit Determination

The carrier-only kinematic solution is more than a curiosity. It will allow accurate orbit determination with simple codeless receivers, bypassing the effects of anti-spoofing, and can bc used to achieve fair orbit accuracy with single-frequency data as well (Yunck, 1992), In the examples thus far wc've assumed dual-frequency elimination of ionospheric delay; but the ionosphere can also be removed by averaging the L1 phase and pseudorange observables. Consider these simplified expressions for the phase and group delay (pseudorange) observables :

$$\tau_\phi \cong \tau - \frac{k \bullet TEC}{f^2} + bias + \varepsilon_\phi \qquad (35)$$

and

$$\tau_{grp} \cong \tau + \frac{k \bullet TEC}{f^2} + \varepsilon_{grp} \qquad (36)$$

where TEC is the total electron content along the raypath, f is the observing frequency, k is a constant, ε is the random measurement error, and τ is the common delay due to geometry and other factors besides the ionosphere. Note that the ionospheric term is identical in both equations but appears with opposite sign. Forming the simple average of (35) and (36) wc obtain

$$\frac{\tau_\phi + \tau_{grp}}{2} \cong \tau + \text{bias}' + \frac{\varepsilon_\phi + \varepsilon_{grp}}{2} \qquad (37)$$

The ionospheric term is cancelled and the resulting, observable has the form of the biased carrier phase delay (35). Because ε_{grp} is much greater than ε_ϕ, the effective measurement error on (37) is half that of pseudorange. This is sometimes called the GRAPHIC (GRoup Anti PHase Ionospheric calibration) observable. Note that the conventional dual-frequency correction *increases* raw data noise by a factor of three; thus if single-frequency phase is 100 times more precise than pseudorange, dual-frequency phase will be only 16 times more precise than the GRAPHIC observable.

Modern receivers that employ 20 MHz C/A-code processing can recover C/A pseudorange with a precision of better than 50 cm in 1 sec. The GRAPHIC observable reduces this by half. Smoothing over 60 sec can bring the error below 10 cm. Figure 8 shows the predicted 3-D RMS position error for the Shuttle at 300 km with three solution strategies: dual-frequency dynamic, GRAPHIC kinematic, and dual-frequency kinematic. Key assumptions are shown in Table 4. Note that drag and gravity errors make the dynamic solution worse than simple point positioning. The kinematic solutions improve orbit accuracy by two to three orders of magnitude, reaching about 2 cm per component with dual-frequency phase. The order-of-magnitude difference between the two kinematic cases is explained by the higher data noise on the GRAPHIC observable, which was assumed at all ground sites as well.

Single-freqLlcncy ionospheric calibration was demonstrated for the first time on an earth satellite by Gold et al (1993). The Extreme Ultraviolet Explorer (EUE), flying at about 500 km, is equipped with a 12-channel L1 -only receiver and two oppositely directed antennas, providing a full sky field of view. Many GPS tracks acquired by EUE look down through the ionosphere, where the added delay can exceed 50 m. Figure 9 presents typical postfit residual plots for EUE GPS orbit solutions with both uncorrected 1.1 phase (a) and the inherently noisier but ionosphere-corrected GRAPHIC observable (b). In the latter case, large ionospheric excursions are entirely absent. Direct comparison of orbit overlaps indicates an RMS altitude error of less than 1 m in a differential reduced dynamic EUE solution with the singic-frequency GRAPHIC observable.

e) Extension to Higher A ltitude Satellites

Above about 3000 km, an orbiter begins to lose coverage from GPS. But since dynamic modeling error can be small at high altitudes, the dynamic orbit solution can remain strong. By looking downward to catch the signal spillover from satellites on (he other side of the earth, an orbiter can exploit GPS from well above the GPS satellites themselves, out to geosynchronous altitude and beyond. Alternatively, high satellites can carry GPS-like beacons to be tracked from the ground, with the GPS satellites serving as reference points, a technique known as *inverted GPS*. Figure 10 (from WLI et al., 1992) plots the average number of GPS satellites that can be tracked by a circular orbiter as a function of altitude, for both upward- and downward-looking vehicles, where each is assumed to have a hemispherical field of view. Note that above about 2000 km, the down-looking user can always track more. The figure also plots the average number of ground sites that can track a beacon on a circular orbiter, assuming a (en-site global network.

A study of direct orbit determination with down-looking GPS (Wu et al., 1992) was carried out for NASA's geosynchronous Tracking and Data Relay Satellites (TDRS). With GPS orbit error assumed to be 7 m and clock error 2 m (SA off), a predicted 3-D TDRS position accuracy of 12 m is reached dynamically after 8 hrs, improving to 9 m after 24 hrs. With SA assumed on, the error jumps to over 100 m at 8 hrs, declining to 60 m at 24 hrs.

A ground network of a dozen sites can now easily provide sub-meter GPS orbit accuracy. If those receivers were to track an additional high altitude beacon, all orbits could be estimated in one solution with comparable relative accuracy, scaled for distance. Wu et al. (1992) examined this inverted GPS tracking for TDRS as well. With assumed data errors of 25 cm for pseudorange and 1 cm for carrier phase at 30 min intervals, and a six-site ground network, the predicted 3-D RMS orbit error over a 24-hr dynamic solution arc was about 3 m for the TDRS satellites.

f) Highly Elliptical Orbiters

Since the preferred tracking modes and solution techniques differ for high and low orbiters, the application to highly elliptical orbiters, which may descend to a few hundred kilometers and rise to tens of thousands, present a special challenge. Up- and down-looking GPS combined with ground-based Doppler during the high altitude phase can provide particularly strong coverage. The proposed MUSES-B spacecraft, part of the Japanese very long baseline interferometry (VLBI) Space observatory Program, was studied by Wu et al. (1992). MUSES-B would move from a perigee of 1000 km to an apogee of 20,000 km. The investigators applied a reduced dynamic strategy while the satellite was below 2000 km, and a purely dynamic strategy elsewhere. Combined omnidirectional differential GPS and ground-based Doppler gave a predicted orbit error of 50 cm for all position components at apogee, falling to less than 10 cm at perigee.

A similar mission, the proposed International VLBI Satellite, would have a perigee of 5000 km, enabling a purely dynamic solution around the orbit, Wu et al. (1992) found that with omnidirectional differential GPS and ground-based Doppler, as the apogee increases from 40,000 to 150,000 km, position error at apogee increases from about 15 cm to over 2 m. Such accuracy is needed for only a select group of missions, Direct GPS orbit determination with omnidirectional reception could provide 10 m or better accuracy for nearly all highly elliptical orbiters.

6. Dealing with Selective Availability and Anti-Spoof

The two GPS security features, selective availability (SA) and anti-spoofing (AS), can pose problems for SPS users. Over the years, various strategies have been devised to address them.

a) Anti-Spoofing

Anti-spoofing is the encryption of the P code to prevent mimicking of the signal by others. In the presence of AS, a conventional SPS receiver would be able to track only the C/A code, recovering pseudorange and carrier phase on L1 only. This would prohibit computation of the standard dual frequency ionospheric correction. The ionospheric effect of course depends on the altitude and field of view of the user. Above about 1000 km (and assuming an upward-directed hemispherical field of view), the rare ionosphere permits sub-meter single-frequency orbit accuracy, even with no

correction. At lower altitudes, as shown on EUE, the GRAPHIC calibration used in a reduced dynamic differential solution can give an orbit accuracy of about 1 m. That approach holds promise in both real time and post-processing uses for all but the most demanding requirements.

Low orbiters seeking sub-decimeter performance must turn to dual frequency calibration. 'I'here are several GPS receiver designs that ope.rate in a codeless or quasi -codeless mode; that is, they produce carrier phase (and, in some cases, pseudorange) at both frequencies without knowledge of the precise codes. Although codeless data arc of degraded precision, the typical codeless phase error of about 1 cm in 1 sec is consistent with the assumptions used in the studies presented here. Phase measurement noise, moreover, is generally not the dominant error in an orbit solution. Tracking performance will therefore be largel y unaffected by a switch to codeless operat ion.

b) Selective A vailability

SA consists of two measures to degrade positioning accuracy to the unauthorized user: the insertion of errors into the broadcast ephemeris and clock parameters, and "dithering" of the fundamental oscillator. Neither of these measures poses a problem for differential GPS tracking as wc have defined it here. Receiver sampling times can be synchronized so that dither effects arc common to all measurements and drop out of the differential solution. When sampling is not synchronized, quadratic interpolation to a common epoch can still achieve a high degree of dither cancellation provided the sampling interval is no longer than about 30 sec (Wu et al, 1990). Ephemeris and clock errors do not come into play since those quantities are solved for with the ground data, either together with the user orbit or in advance.

Real lime direct GPS users encounter more difficulty. Those without access to accurate GPS orbits computed elsewhere will have to rely primarily on dynamic smoothing to reduce the effects of both the orbit error and dithering. At nominal SA levels, the broadcast orbit error is 40 m or less on each satellite. (In recent years, in fact, the broadcast ephemeris has remained uncorrupted even when dither is active.) From the vantage of the user, the corrupted orbits will appear to some degree inconsistent with the GPS measurements and the user's dynamics-and the dynamic solution will then attenuate GPS orbit error. Early studies suggest that the error reduction will be about a factor of two. A 40 m GPS errors may yield a 20 m user error. The actual reduction will depend on the solution strategy, receiver capacity, field of view, and other factors.

Smoothing of dither error by dynamic filtering has been more thoroughly analyzed. Bar-Sever et al. (1990) simulated the dither process to examine the error reduction as a function of dynamic arc length. Figure 11 shows the net 3-D error (due to dither only) for smoothing periods ranging from zero (point positioning) to 6 hrs. The receiver is assumed to track all satellites within a hemisphere and dither is set at its nominal level. We scc that with no smoothing, the RMS dither error is about 30 m. After 2 hrs this falls to 5 m, and after 6 hrs to less than 3 m.

A satellite like Topex/Poseidon, which has well modeled dynamics, can realize the full benefit of dynamic SA smoothing. At altitudes below about 600 km, dynamic model error will begin to offset the gain from smoothing, and at typical Shuttle altitudes the optimal direct solution may be little better than the point position solution under SA. To improve real time accuracy at low altitudes, some form of near-rca] time correction must be applied. This could be carried out, as is

now commonly done for air and surface navigation, with pseudorange corrections derived at reference sites broadcast directly to users. Systems may soon be in place to send such corrections over wide areas through geosynchronous satellites (see Vol. 1, Ch. 21). A low orbiter equipped to receive those corrections could then achieve real t imc posit ion accurac y of a few meters under SA.

7. Summary

The positioning strength provided by GPS is transforming Earth satellite orbit determination. With even the simplest receiving equipment it is now possible to determine (he position of a low orbiter instantaneously to tens of meters, sufficient to meet the needs of most missions. The classical framework of dynamic orbit estimation can be adapted for GF%-equipped satellites in virtually any orbit to deliver orbit accuracies beyond the previous state of the art. Many low Earth satellites now in the planning stages will carry GPS for basic navigation and timing, and in some cases for direct scientific uses. Before GPS, orbits below 700 or 800 km could not be considered for altimetric satellites seeking accuracies of a decimeter or better. GPS promises to deliver fcw-centimeter accuracy at the lowest altit udes and for the most dynamically ill-behaved platforms. This creates the opportunity for low-power, low-mass, low-cost altimetry at an altitude of a few hundred kilometers, and for demonstrating precise sensing instruments on the Space Shuttle.

Figure 12 summarizes the performance that can be achieved as a function of altitude for both real time direct and after-the-fact differential GPS-based orbit determination. The curves reflect the optimal estimation strategy for each case. For satellites above 10,000 km the standard differential technique is replaced by inverted GPS, where the orbiter carries a beacon tracked from the ground. The differential curve is consistent with the assumption of a dual frequency codeless (S1%) receiver and is therefore unaltered by the presence of SA (eliminated by differencing) or AS. All curves for direct estimation assume the use of high quality (2-3 m) GPS orbits and clocks distributed by civilian services, rather than the broadcast ephemeris, Thus only dither error is included in the SA-on case. These curves are necessarily approximate, as actual performance will depend on specifics of the GPS tracking configuration and satellite dynamics. But they offer a view of the new standard GPS brings to orbit determination for missions of every description.

Acknowledgement

Portions of the work described in this chapter were carried out by the Jet Propulsion laboratory, California Institute of Technology, under contract with the National Aeronautics and Space Administration.

References

Axelrad, P. and J. Kelley (1986), Near earth orbit determination and rendezvous navigation using GPS, *Proc. IEEE PLANS '86,* Las Vegas, Nov 4-7, pp. 184-191.

Axelrad, 1'. and B. W. Parkinson (1989), Closed loop navigation and guidance for Gravity Probe B orbit insertion, *Navigation, 36, pp45-61.*

llar-Sever, Y., T, P. Yunck and S. C. Wu (1990), GPS mbit determination and point positioning under selective availability, Pmt. ION GPS-90, Colorado Springs, CO, pp. 255-265.

Bertiger, W, I. and T. P. Yunck (1990), The limits of' direct satellite tracking with GPS, *Navigation,* 37, pp. 65-79.

Bierman, G. J. (1977), *Factorization Methods for Discrete Sequential Estimation*, Academic Press, Orlando, FL, 241 pp.

Chao, C. C., }1. Bernstein, W. H. Boyce and R. J. Perkins (1992), Autonomous stationkeeping of geosynchronous satellites using a GPS receiver, AlAA 92-4655, *Proc. AIAA/AAS Astrodynamics Conf.*, Hilton Head Is., SC, Aug 10-12, pp. 521-529.

Fang, B. T. and E. Seifert, An evaluation of Global Positioning System data for Landsat-4 orbit determination, AIAA 85-0286, AIAA Aerospace Sciences Meeting, Reno, NV, Jan 14-17,9 pp.

Farr, J. E. (1979), Space navigation using the Navstar Global Positioning System, AAS 79-001, Rocky Mountain Guidance and Control Conference, Keystone, CO, Feb 24-28, 27 pp.

Gold, K., W. 1. Bertiger, S. C. Wu and T. P. Yunck (1993), Preliminary GPS orbit determination results for the Extreme Ultraviolet Explorer, paper AAS-93-157, AAS/AIAA Spaceflight Mechanics Meeting, Pasadena, CA.

Hesper, E. T., B. A. C. Ambrosius, R. J. Snijders and K. F. Wakker (1992), Application of GPS for Hermes rendezvous navigation, *Spacecraft Guidance, Navigation and Control Systems*, European Space Agency, pp. 359-368.

Heuberger, H and 1.. Church (1983), Landsat-4 Global Positioning System navigation results, AAS 83-363, *Proc. AAS/AIAA Astrodynamics Conf.*, Part 1, Lake Placid, NY, Aug 22-25, pp. 589-602.

Jorgensen, P. (1982), Autonomous navigation of geosynchronous satellites using the Navstar Global Positioning System, Proc. NTC'82, National Telesystems Conf., Galveston, TX, Nov 7-10, pp. 112.3.1 -D2.3.6.

Kurzhals, I'. S. and A. J. Fuchs (1981), Onboard navigation - The near-earth options, Proc. Rocky Mountain Guidance and Control Conference, Keystone, CO, Feb 17-21, pp. 67-89.

Lichten, S. M. (1990), Estimation and filtering for high-precision GPS positioning applications, *Manuscripta Geodaetica,* 15, pp. 159-176.

Lichten, S. M. and W. I. Bertiger (1989), Demonstration of sub-meter GPS orbit determination and 1.5 parts in 108 three-dimensional baseline accuracy, *Bull. Géodesique,* 63, pp. 167-189.

Lichten, S. M., C. D. Edwards, L. E. Young, S. Nandi, C. Dunn and B. J. Haines (1993), A demonstration of TDRS orbit determination using differential tracking observable from GPS ground receivers, AAS 93-160, Third AAS/AIAA Spaceflight Mechanics Meeting, Pasadena, CA, Feb 22-24.

Masson, B. L., M. P. V. Ananda and J. Young (1982), Functional requirements of the next generation spaceborne Global Positioning System (GPS) receivers, Proc. IEEE National Telesystems Conf., Galveston, TX, 9 pp.

Munjal, l)., W. Feess and M. Ananda (1992), A review of spaceborne applications of GPS, Proc. ION GPS-92, The Institute of Navigation, 16-18 Sept, pp. 813-823.

Ondrasik, V. J. and S. C. Wu, A simple and economical tracking system with sub-decimeter Earth satellite and ground receiver position determination capabilities, Proc. 3rd Int. Symp. on the use of Artificial Satellites for Geodesy and Geodynamics, Ermioni, Greece, Sept.

Parkinson, B. W. (1976), Navstar global positioning (GPS), Proc. National Telecomm. Conf., Nov.

Rosborough, G. and S. Mitchell (1990), Geographically correlated orbit error for the Topex satellite using GPS tracking, AIAA 90-2956, Pmt. *AIAA/AAS Astrodynamics Conf., Part 2*, Portland, OR, Aug 20-22, pp. 655-663.

Schreiner, W. S., G. }[. Born, K. M. Larson and P. F. MacDoran (1992), Error analysis of post-processed orbit determination for the Geosat Follow-On altimetric satellite using GPS tracking, AIAA 92-4435, *Proc. AIAA/AAS Astrodynamics Conf.*, Hilton Head Is., SC, Aug 10- 12, pp. 124-130.

Schutz, B. E., B. D. Tapley, P. A. M. Abusali and H. J. Rim (1993), Dynamic orbit determination using GPS measurements from Topex/Poseidon, *Geophys. Res. Lett.*, submitted Aug 1993.

Tapley, B. D. (1980), A study of autonomous satellite navigation methods using the Global Positioning System, Report #: NASA-CR- 162635, Dept. of Aerospace and Engineering, University of Texas at Austin, 55 pp.

Thornton, C. L. (1976), Triangular covariance factorization for Kalman filtering, JPL Internal Document, TM 33-798, Jet Propulsion Laboratory, Pasadena, CA.

Van Leeuween, A., E. Rosen and L. Carrier (1979), The Global Positioning System and its applications in spacecraft navigation, *Navigation, 26,* pp. *204-221.*

Wooden, W. H. and J. Teles (1980), The Landsat-D Global Positioning System experiment, AIAA 80-1678, AIAA/AAS Astrodynamics Conf., Danvers, MA, Aug. 11 -i 3, 10 pp.

WLI, J. 1'. (1984), Elimination of clock errors in a GPS based tracking system, paper AIAA-84-2052, AIAA/AAS Astrodynamics Conference, Seattle, WA.

WU, J. T. (1992), Orbit determination by solving for gravity parameters with multiple arc data, *J. Guidance, Control and Dynamics, IS,* pp *304-313.*

Wu, S. C. (1985), Orbit determination of high-altitucic Earth satellites: Differential CiPS approaches, *Proc. 1st Int. Symp. on Precise Positioning with the Global Positioning System*, Rockville, MD, Apr.

WU, S. C., W. I. Bertiger, J. S. horder, S. M. Lichten, R. F. Sunseri, B. G. Williams, P. J. Wolff and J. T. Wu (1986), *OASIS Mathematical Description, v. 1.0,* J}']. Internal Document D-3139.

WU, S. C., T. P. Yunck, C. L. Thornton (1991), Reduced-dynamic technique for precise orbit determination of low earth satellites, *J. Guidance, Control and Dynamics, 14,* pp. *24-30.*

Wu, S. C., W. I. Bertiger and J. T. Wu (1990), Minimizing selective availability error on Topex GPS measurements, AIAA paper 90-2942, AI AA/AAS Astrodynamics Conference, Portland, OR.

Wu, S. C., T. P. Yunck, S. M. Lichten, B. J. Haines and R. P. Malla (1992), GPS-based precise tracking of Earth satellites from very low to geosynchronous orbits, Proc. National Telesystems Conference, Ashburn, VA.

Yunck, T. F'. and W. G. Melbourne (1989), Geoscience from GPS tracking by Earth satellites, in Bock, Y. and N. Leppard, eds., *Global Positioning System: An Overview*, IUGG Symposium 102, Springer-Verlag, New York.

Yunck, T. P., W. G. Melbourne and C. 1.. Thornton (1985), C,} 'S-based satellite [racking system for precise positioning, *IEEE Trans. Geosci. and Remote Sensing*, GE-23, July, pp. 450-457.

Yunck, T. P., S. C. Wu, J. T. Wu and C. L. Thornton (1990), Precise tracking of remote sensing satellites with the global positioning system, *IEEE Trans. Geosci. & Remote Sensing,* 28, pp. 108-116.

Yunck, 1'. P. (1992), Coping with the atmosphere and ionosphere in precise satellite and ground positioning, in Jones, A. V., cd., *Environmental Effects on Spacecraft Trajectories and Positioning*, IUGG Union Symposium 15, Springer-Verlag, New York, in press.

Yunck, T. P. (1993), W. 1. Bertiger, S. C. Wu, Y. Bar-Sever, E. J. Christensen, B. J. Haines, S. M. Lichten, R. J. Muellerschoen, Y. Vigue and P. Willis, First assessment of GPS-based reduced dynamic orbit determination on Topex/Poseidon, *Geophys. Res. Lett.*, submitted Aug 1993.

TABLE 1. Error Model for Topex/Poseidon Orbit Determination Analysis

System Characteristics	
Orbit (circular):	1334km, 66° inclination
Number of Ground Sites:	6 (including 3 fiducial sites)
Number of GPS Satellites:	18
Flight Antenna Field of View:	Hemispherical
Flight Receiver Tracking Capacity:	6 Channels (L1& 1.2)
Data Types:	L1 & L2 pseudorange
	L1& 1.2 carrier phase
Data Interval:	5 Minutes
Smoothed Data Noise:	5 cm pseudorange
	1 cm carrier phase
Adjusted Parameters & A Priori Errors	
Topex/Poseidon Epoch State:	1km; 1 n]/see, each component
GPS Satellite States:	2 m; 0.2 mnl/see, each component
Carrier I'base Biases:	10 km
GPS & Receiver Clock Biases:	3 msec (modeled as white noise)
Non-Fiducial Ground Locations:	20 cm each component
Fixed Errors Evaluated	
Fiducial Site Positions:	5 cm each component
GM of Earth Uncertainty:	1 part in 10^8
1 Earth Gravity Error Model:	0- 100% GEM10-GEML2 (20x20)
Zenith Atmospheric Delay Error:	1 cm (modeled as random walk)
Atmospheric Drag Error:	10% of Total
Solar Radiation Pressure Error:	10% of Total

TABLE 2. Changes from Table 1 for Earth Observing System Kinematic Orbit Determination Analysis

Orbit (circular):	705 km, 98° inclination
Number of GPS Satellites:	24
Flight Receiver Tracking Capacity:	All in View (within hemisphere)
Zenith Atmospheric Delay Error:	Adjusted as Random Walk
Fiducial Location Error:	3 cm each component
Earth Gravity Error Model:	100% GEM10-GEML2 (20x20)

TABLE 3. Changes from Table I for Shuttle
Kinematic Orbit Determination Analysis

Orbit (circular):	300 km, 28° inclination
Number of GPS Satellites:	24
Number of Ground Sites:	11 (including 3 fiducial sites)
Flight Antenna Field of View:	Full Sky
Flight Receiver Tracking Capacity:	All in View
Smoothed Data Noise:	5 cm pseudorange 5 mm carrier phase
Zenith Atmospheric Delay Error:	Adjusted as Random Walk
Fiducial Location Error:	1.5 cm each component
Earth Gravity Error Model:	50%GEM10-GEM12 (20x20)

TABLE 4. Key Assumptions for Shuttle Single-Frequency
Kinematic Orbit Determination Analysis

Orbit (circular):	300 km, 98° inclination
Number of GPS Satellites:	24
Number of Ground Sites:	6 (including 3 fiducial sites)
Flight Receiver Tracking Capacity:	All in View (within hemisphere)
Smoothed Data Noise:	10 cm pseudorange (single-freq.) 1 cm carrier phase
Zenith Atmospheric Delay Error:	Adjusted as Random Walk
Fiducial Location Error:	3 cm each component
Earth Gravity Error Model:	50%GEM 10-GHM1,2 (20x20)
Atmospheric Drag Error:	10% of Total

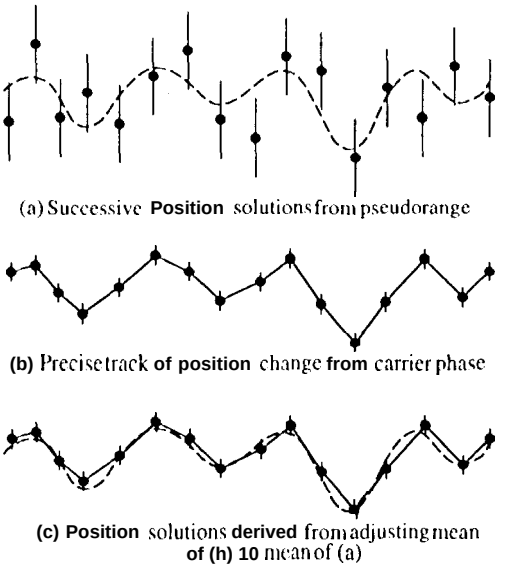

Fig. 1. In carrier-pseudorange point positioning, the bias in carrier-based position measurements is estimated by averaging the difference between carrier and pseudorange solutions. The result retains the precision and time resolution of the carrier solution, with a small residual bias.

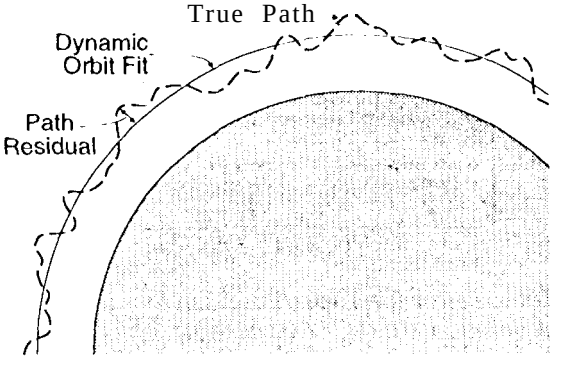

Fig. 2. The. kinematic orbit determination technique effectively reconstructs the observed trajectory from the residuals of a dynamic orbit solution.

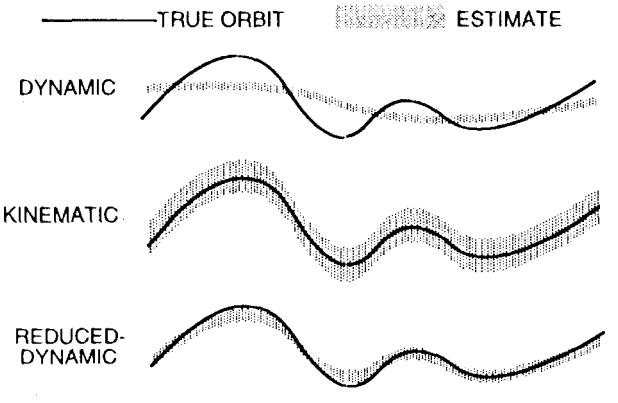

Fig. 3. The purely dynamic orbit solution minimizes the contribution of random error, while dynamic model error is fully expressed; this is reversed in the kinematic solution. The reduced dynamic solution yields an intermediate level of each error and can minimize. overall error.

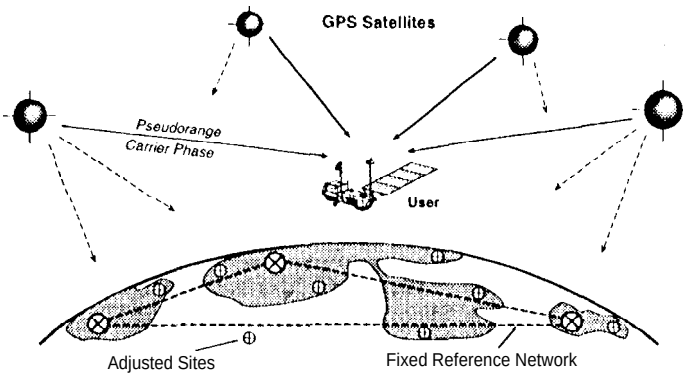

Fig. 4. In precise orbit determination with differential H'S, user and ground observations of GPS arc combined to determine user, GPS, and some ground positions with respect to a subset of ground reference or "fiducial" sites.

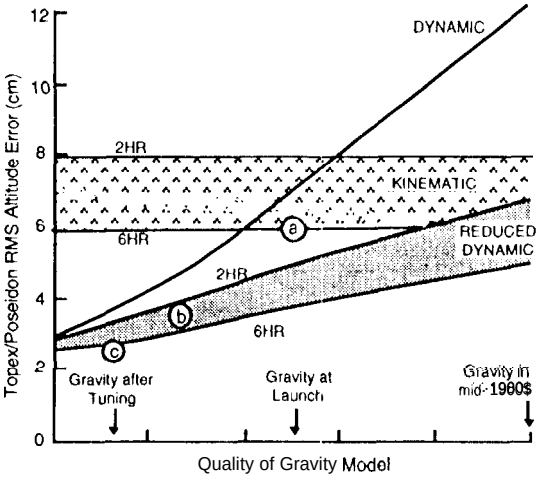

Fig. 5. Predicted RMS altitude error for Topex/Poseidon as a function of the quality of the gravity model, for three different solution strategies (see Table 1). Circles show actual RMS altitude agreement between GPS reduced dynamic and laser/Doppler dynamic solutions made with the prelaunch gravity model (a), a laser/Doppler-tuned model (b), and a GPS-tuned model (c).

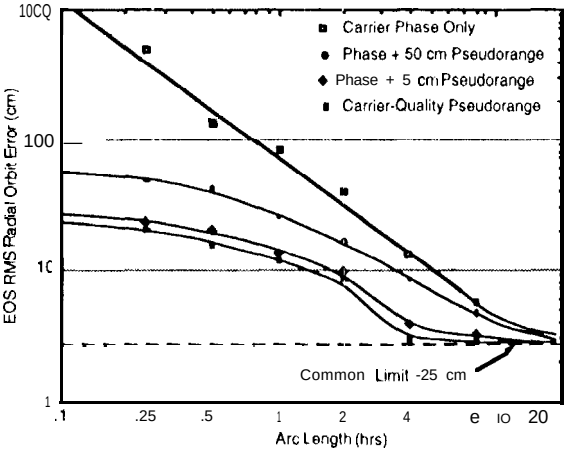

Fig. 6. Predicted RMS altitude error for EOS as a function of data arc length, for purely kinematic orbit determination and four data combinations. Key assumptions are shown in Table 2.

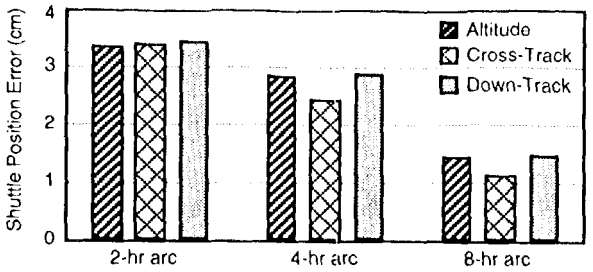

Fig. 7. Predicted kinematic tracking error for the Space Shuttle with a robust GPS observing system. Key assumptions are shown in Table 3.

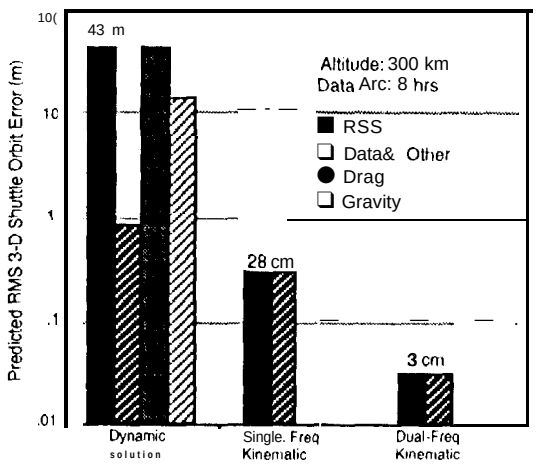

Fig. 8. Predicted 3-1) position error for the Space Shuttle at 300 km, with three solution strategies

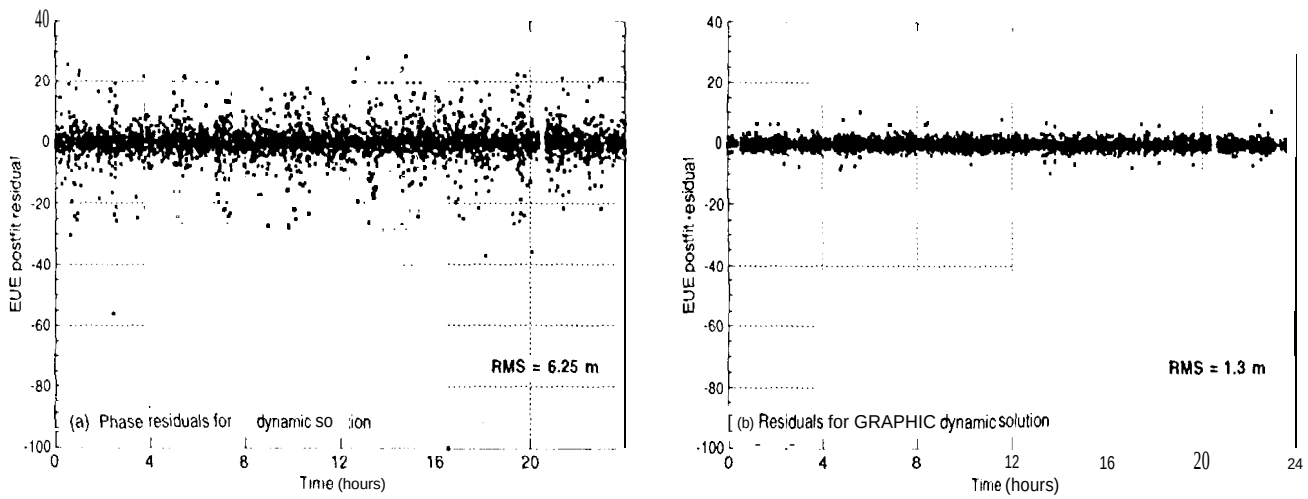

Fig. 9. Postfit residual plots for GPS-based EUE dynamic orbit solutions with single-frequency carrier phase data (a) and the single-frequency ionosphere calibrated GRAPHIC observable (b).

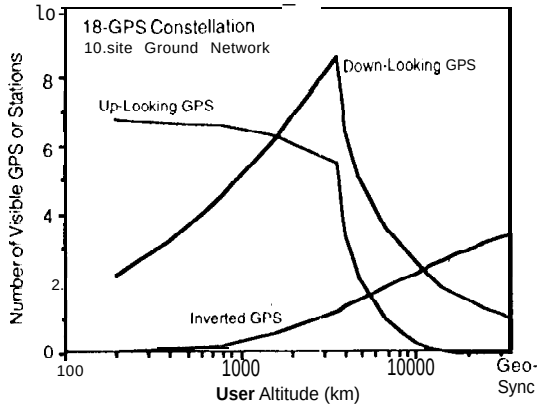

Fig. 10. Average numbers of GPS satellites visible with upward and downward looking hemispherical antennas, and average. number of sites from a lo-site ground network that can track an orbiting beacon, as a function of altitude.

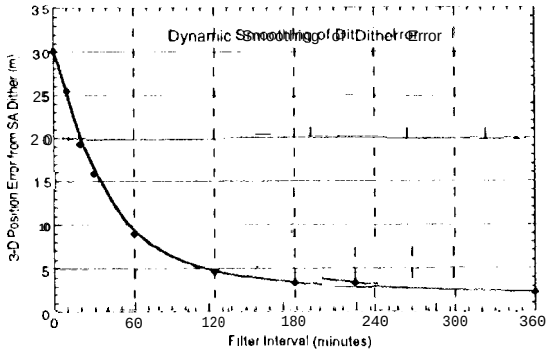

Fig. 11. Simulation results showing the 3-D position error that results from SA dithering, set at its nominal level, as a function of dynamic smoothing interval. No other errors are shown.

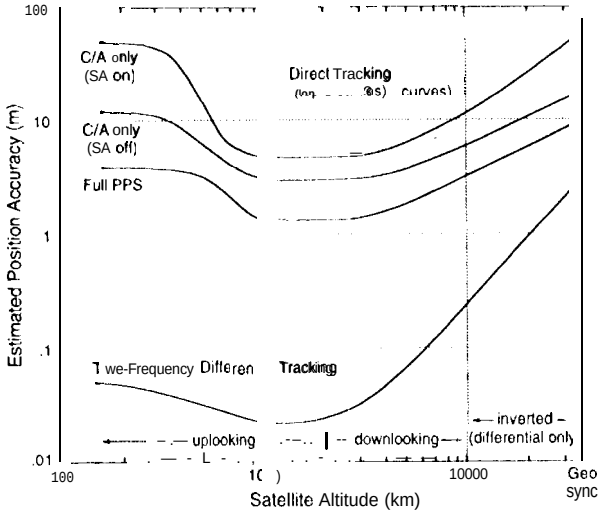

Fig. 12. Summary of the estimated orbit accuracies currently achievable with both differential and real time direct GPS techniques. The direct solutions assume the use of precomputed GPS orbits of 2-3 m accuracy.